Supplementary materials & methods

Wound-healing assay

Cells were grown in six-wells plates with DMEM containing 10% FBS until 90% confluence. A "wound" was made via scratching with a pipette tip. After cultured in medium without FBS for 48 h, cell migration was observed using light microscopy. The migration distance of cells at the same position was measured by using Image-Pro Plus software. All experiments were independently repeated three times.

Transwell migration assay

Cells (1×10^4) were seeded in 8-μm cell culture inserts (Corning Incorporated, Corning, NY, USA) in DMEM without FBS and incubated in 24-well plates with 10% FBS supplemented with DMEM for 16 h. Transmigration cells were stained with 0.1% crystal violet. Photographs of five randomly selected fields of the fixed cells were captured, and cells were counted. Experiments were independently repeated three times.

Xenograft model

Animal experimental protocols were approved by the Animal Care and Use Committee of Shanghai Jiao Tong University School of Medicine. Six- week-old male nude mice (BALB/c) were housed six mice per cage in a specific pathogen-free room with a 12-hr light/dark schedule at 25°C±1°C and were fed an autoclaved chow diet and water ad libitum. The mice were randomly divided into indicated groups (6-8 mice/group) before inoculation, Tumor tissue masses from *Gpr110*$^{-/-}$ mice and wild-type mice were subcutaneously injected into the mice to form the subcutaneous model, the volume of every mass is about 2 mm^3 and one nude mouse was injected two masse, tumor growth was monitored every 4 days. Mice were sacrificed after one month and their tumor were removed. Tumor were fixed with paraform aldehyde (4%) before dehydration and embedding in paraffin. Paraffin sections were stained with H&E according to standard protocols.

Statistics

Values presented were expressed as mean ± SD. After acquiring all data for histological parameters and in vitro assays, Student's t-test was applied to determine statistical significance. All statistical tests were two-sided. A value of $p<0.05$ was considered significant.

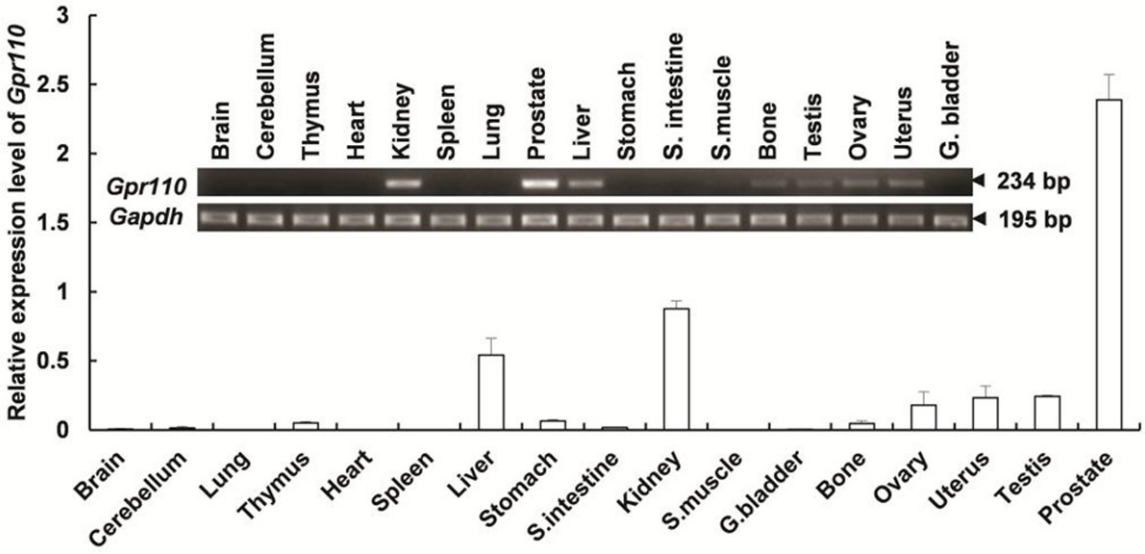

Supplementary Figure 1. Expression profile of *Gpr110* in mice. Semi-quantitative and real-time reverse transcription (RT)-PCR analyses of various mouse tissues. The highest expression level of *Gpr110* mRNA was found in the prostate, while relatively low but detectable expression levels were also observed in the kidney and liver tissues, implicating the tissue compartments where Gpr110 could execute its physiological functions in mice.

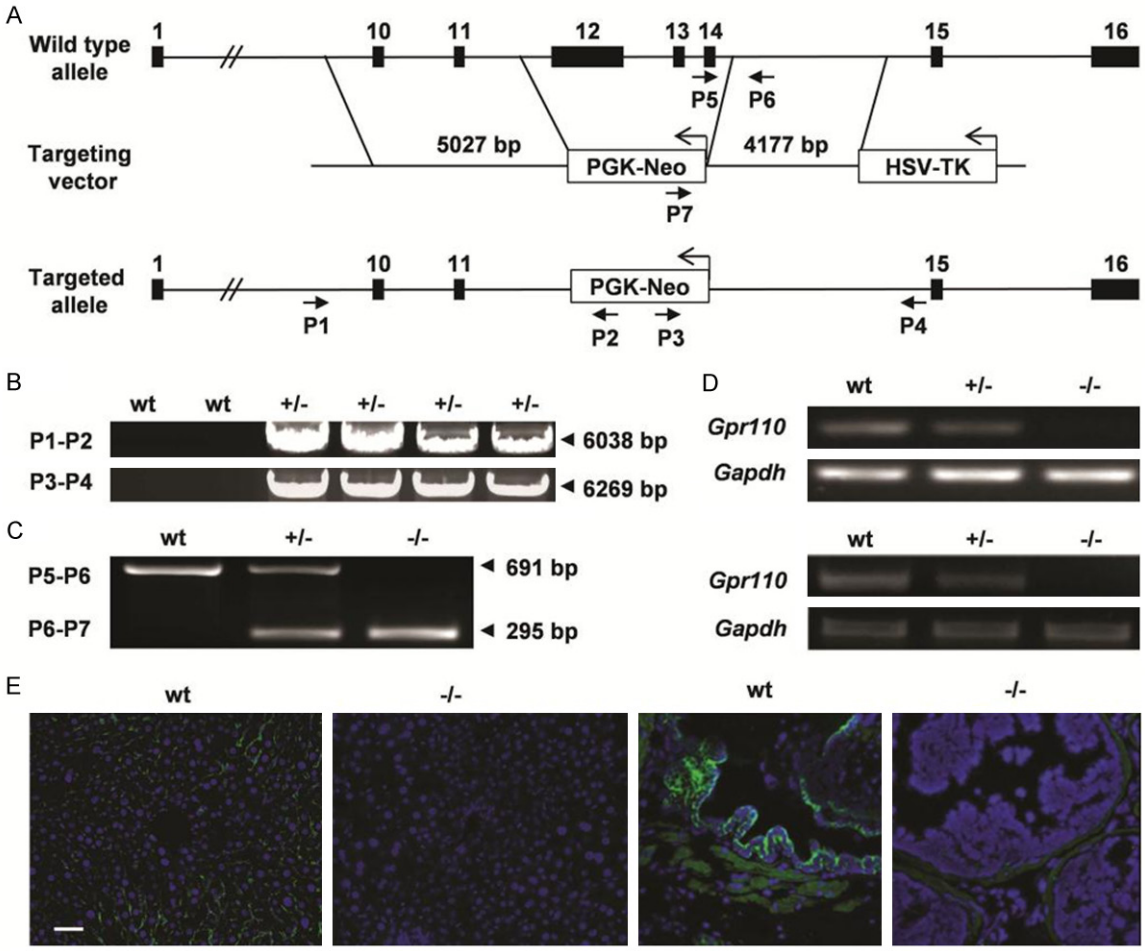

Supplementary Figure 2. Generation of *Gpr110* knockout mice. A. This is the graphic representation of the Gpr110 gene knockout strategy for the deletion of Gpr110 exon 12 to exon 14 in embryonic stem cells. Exons are shown in boxes. The targeting vector was designed to delete exon 12 to exon 14. The targeting vector contained a 5.0 kb 5' arm and 4.2 kb 3' arm. PGK-Neo and HSV-TK cassettes were used for positive and negative selections, respectively. The genomic positive of the PCR primers for genotyping are indicated by arrows. B. Genomic DNA from ES cell clones was isolated and analyzed by PCR with the primers shown in panel A. The successful targeted ES cell clones can be amplified to 6.0 kb and 6.2 kb products for the 5' arm and 3' arm, respectively. C. The PCR analysis for the genotyping of wild-type, *Gpr110*$^{+/-}$ and *Gpr110*$^{-/-}$ mice, showing PCR products of 691 bp from wild-type and 295 bp from targeted alleles. D. Absence of Gpr110 mRNA in the liver tissues (upper panel) and prostate tissues (lower panel) of wild-type, *Gpr110*$^{+/-}$ and *Gpr110*$^{-/-}$ mice detected by using RT-PCR analyses. E. Absence of Gpr110 protein in the liver tissues (left panel) and prostate tissues (right panel) of wild-type and *Gpr110*$^{-/-}$ mice detected by using immunofluorescence analyses. Scale bar, 50 μm.

Supplementary Table 1. Primer pairs for qRT-PCR

Species	Primers	Forward	Reverse
Human	IL-6	CTTCGGTCCAGTTGCCTTCT	GTGCCTCTTTGCTGCTTTCA
	GPR110	ACGCAACCTAGCAATACC	AGCAGCACCACAACGAA
	GAPDH	TGGTATCGTGGAAGGACTCATGAC	ATGCCAGTGAGCTTCCCGTTCAGC
	β-ACTIN	CTGGAACGGTGAAGGTGACA	AAGGGACTTCCTGTAACAATGCA
Mouse	Gpr110	GGGGCTTTGGCATAGGAA	TCGGCTGAGTAACTGTATCTGAGGC
	IL-6	CTTCGGTCCAGTTGCCTTCT	GTGCCTCTTTGCTGCTTTCA
	TNF-α	TCTCATTCCTGCTTGTGGC	CACTTGGTGGTTTGCTACG
	Bcl-XL	GCTTAGCCCTTTTCGAGGAC	CCCACCAGGACTGGATAATG
	Bcl2	GGTGGTGGAGGAACTCTTCA	ACCTACCCAGCCTCCGTTAT
	CYP2E1	TCCCTAAGTATCCTCCGTGAC	CGTAATCGAAGCGTTTGTTG
	IL-1β	AAAAAAGCCTCGTGCTGTCG	GTCGTTGCTTGGTTCTCCTTG
	MIP2	AGTGAACTGCGCTGTCAATGC	AGGCAAACTTTTTGACCGCC
	Mcl-1	CTTATTTCTTTCGGTGCCTTTG	CCAGTCCCGTTTCGTCCTTA
	Socs	AGGGATCTTGTCCTTTGCTG	GGAGAACGTCTTGGCTATGC
	FOXO3A	CTGTCCTATGCCGACCTGA	TGTGCCGGATGGAGTTCTT
	FOXO1	TGAAGAGCGTGCCCTACT	GATTGAGCATCCACCAAGAA
	PIM-1	GCGGCGAAATCAAACTCA	CATCGTGCTCAAACGGAAT
	c-Myc	TGTATGTGGAGCGGTTTCT	GCTGTCGTTGAGCGGGTA
	CyclinD1	GCGTACCCTGACACCAATCTC	CTCCTCTTCGCACTTCTGCTC
	CyclinA	ACATTCACACGTACCTTAGGGA	CATAGCAGCCGTGCCTACA
	β-actin	GGGAAATCGTGCGTGACATT	GCGGCAGTGGCCATCTC

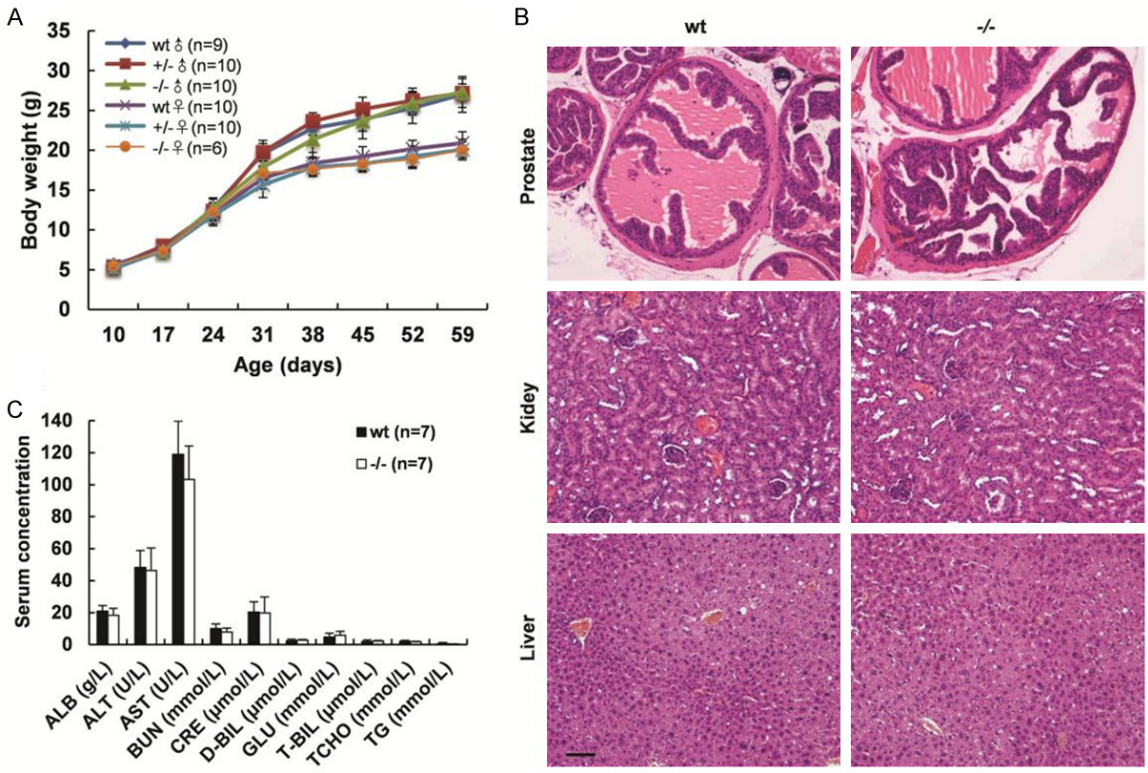

Supplementary Figure 3. *Gpr110*$^{-/-}$ mice were born alive and appeared grossly normal. A. Analysis results showed that the body weight of *Gpr110*$^{-/-}$ offspring mice had no obvious abnormalities. B. Pathological H&E staining of prostate, kidney, and liver in wild-type and Gpr110$^{-/-}$ mice. Scale bar, 100 μm. C. Serum biochemical tests of *Gpr110*$^{-/-}$ mice and wild-type mice. Values are presented as mean ± SD from three independent experiments. **p*<0.05; ***p*<0.01.

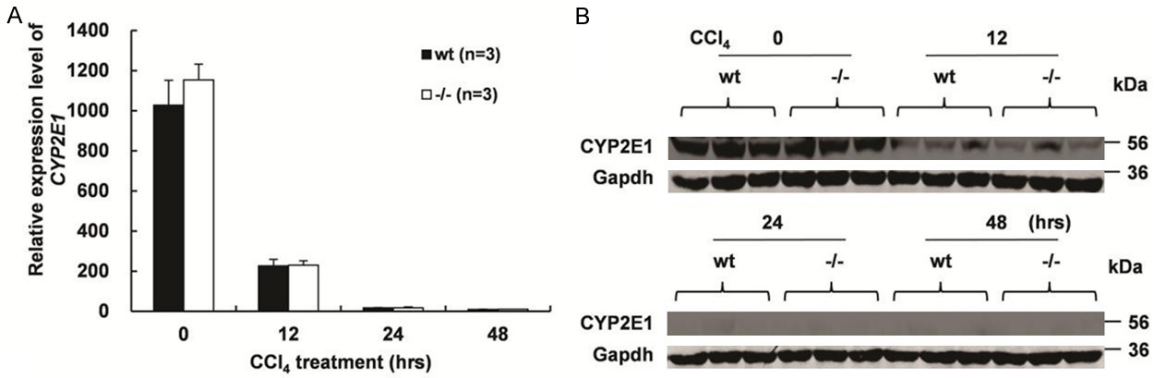

Supplementary Figure 4. The expression of CYP2E1 in liver tissues had no obvious differences between wild-type and *Gpr110*$^{-/-}$ mice. A. Real-time PCR of wild-type and *Gpr110*$^{-/-}$ mice treated with CCl_4 at different time points for expression of CYP2E1. Values are presented as mean ± SD from three independent experiments. **p*<0.05; ***p*<0.01. B. Western blot of wild-type and *Gpr110*$^{-/-}$ mice treated with CCl_4 for different time points for expression of CYP2E1.

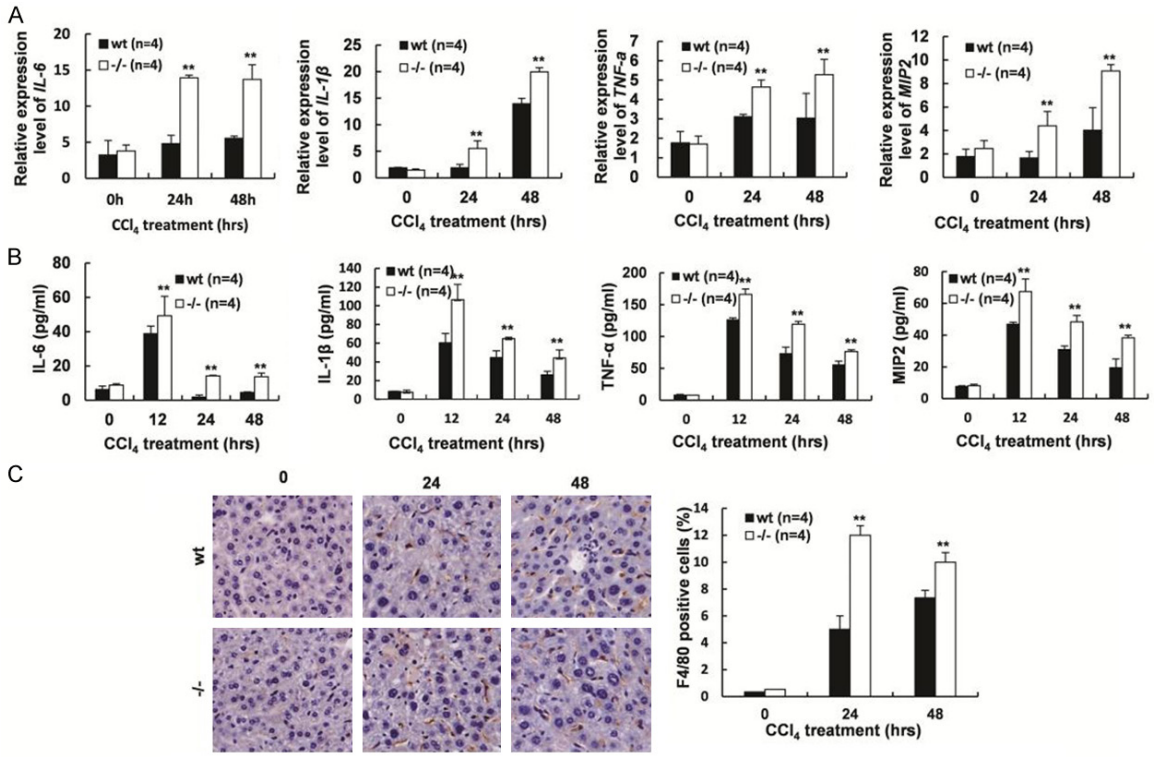

Supplementary Figure 5. Deletion of Gpr110 partially enhanced inflammation after CCl_4 induced acute liver injury. A. qRT-PCR analyses for *IL-6*, *IL-1β*, *TNF-α* and *MIP2* mRNA expression in wild-type and *Gpr110*$^{-/-}$ mice liver treated with CCl_4 for 0 h, 24 h and 48 h (n=4). Values are presented as mean ± SD from three independent experiments. **p*<0.05; ***p*<0.01. B. ELISA analysis of serum levels of IL-6, IL-1β, TNF-α and MIP2 in *Gpr110*$^{-/-}$ mice and wild-type littermates treated with CCl_4 for 0 h, 24 h and 48 h (n=4). Values are presented as mean ± SD. **p*<0.05; ***p*<0.01. C. Immunohistochemical staining of F4/80, sections from 0-, 24- and 48-hours after the CCl_4 injection-sacrificed *Gpr110*$^{-/-}$ mice and wild-type littermate liver (200×), quantified by statistical analyzing percentage of positive cells in 20 high-power fields. Values are presented as mean ± SD. **p*<0.05; ***p*<0.01.

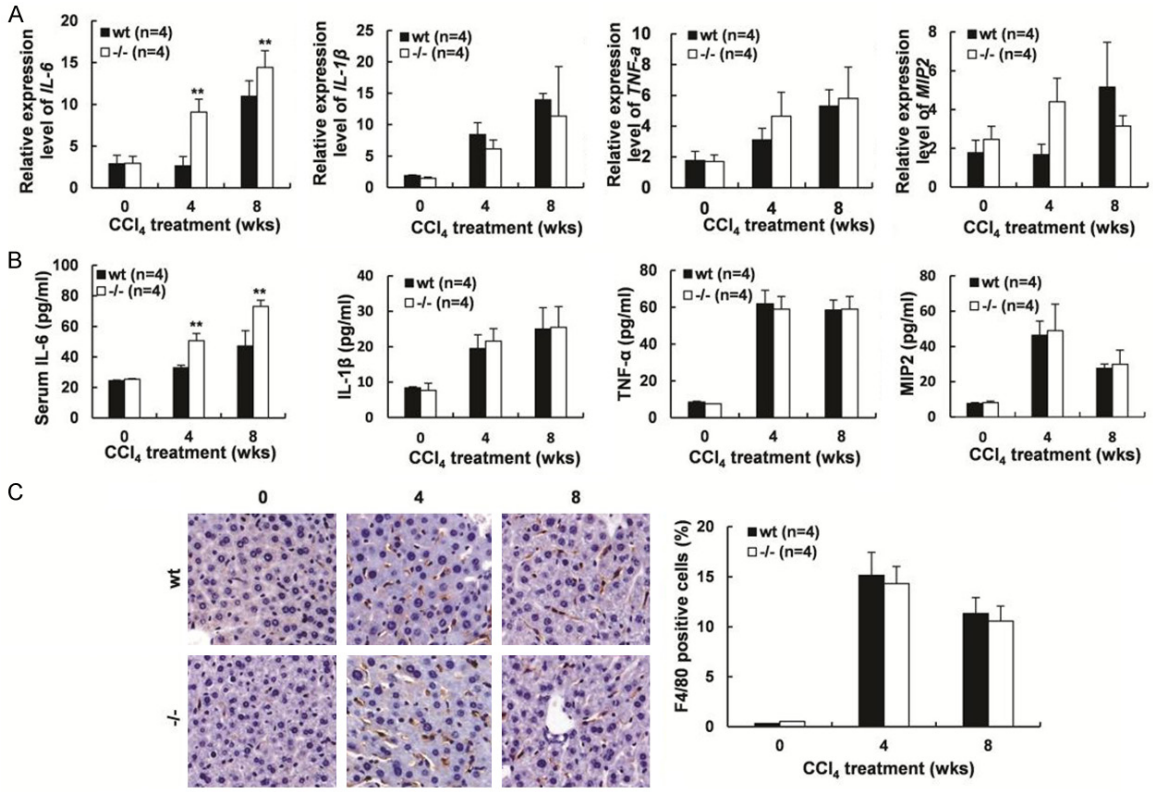

Supplementary Figure 6. Deficiency of Gpr110 did not appear affect inflammation during fibrosis induced by CCl_4. A. qRT-PCR analyses for *IL-6*, *IL-1β*, *TNF-α* and *MIP2* mRNA expression in wild-type and *Gpr110*$^{-/-}$ mice liver treated with CCl_4 for 0 week, 4 week and 8 week (n=4). Values are presented as mean ± SD from three independent experiments. **p*<0.05; ***p*<0.01. B. ELISA analysis of serum levels of IL-6, IL-1β, TNF-α and MIP2 in *Gpr110*$^{-/-}$ mice and wild-type littermates treated with CCl_4 for 0 week, 4 week and 8 week (n=4). Values are presented as mean ± SD. **p*<0.05; ***p*<0.01. C. Immunohistochemical staining of F4/80, sections from 0 week, 4 week and 8 week after the CCl_4 injection -sacrificed *Gpr110*$^{-/-}$ mice and wild-type littermate liver (200×), quantified by statistical analyzing percentage of positive cells in 20 high-power fields. Values are presented as mean ± SD. **p*<0.05; ***p*<0.01.

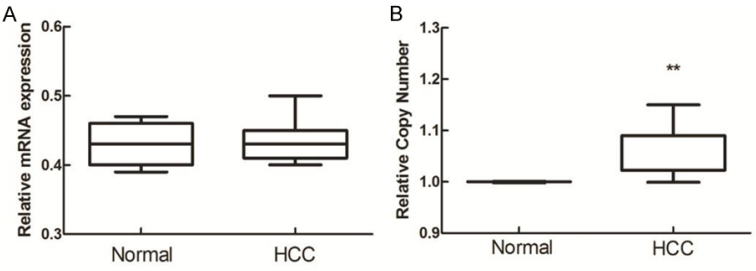

Supplementary Figure 7. The gene copy number of GPR110 rather than the expression of GPR110 in hepatocellular carcinoma was significantly different from the level in normal samples. A. Relative GPR110 mRNA expression in 225 normal and 220 hepatocellular carcinoma samples, no differential expression was observed. (TCGA database, Student t-test, p=0.276). B. Relative GPR110 gene copy number in 115 normal and 97 hepatocellular carcinoma samples, significantly differential copy number was observed. (TCGA database, Student t-test, p=9.84E-8).

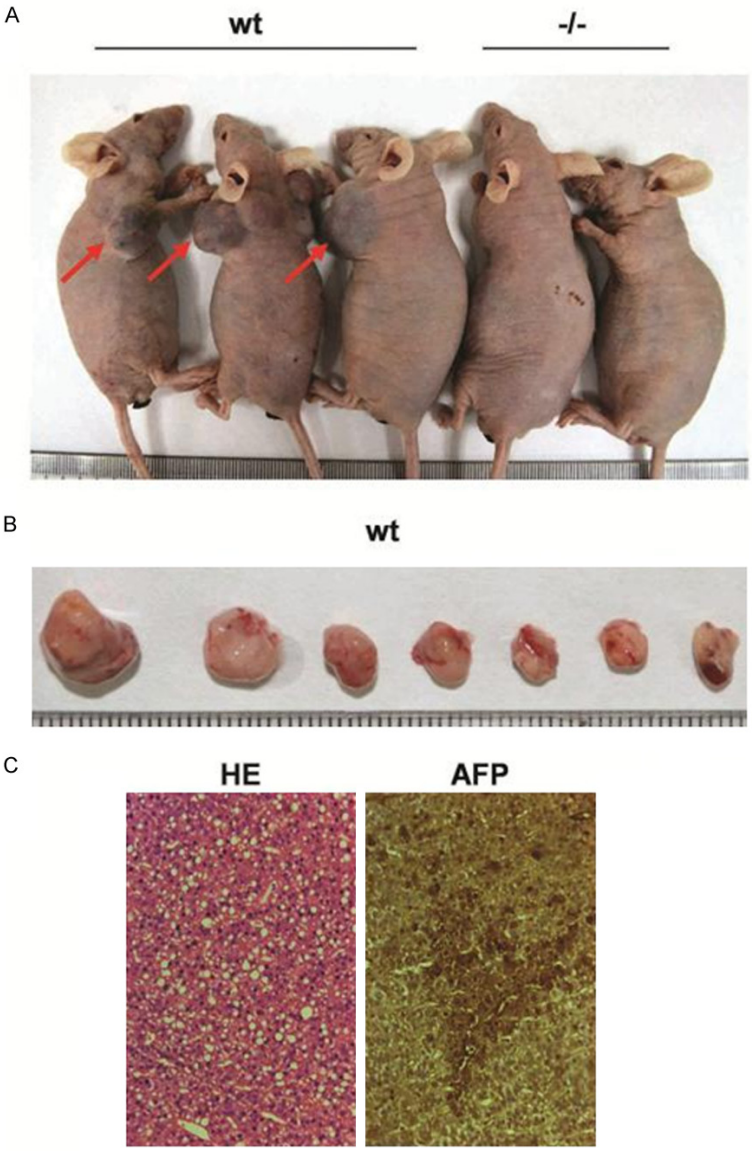

Supplementary Figure 8. Deletion of *Gpr110* in tumor tissue masses significantly reduced tumor growth in the nude mice tumor xenograft model. (A) Representative photographs of nude mice tumor xenograft, tumor tissue masses from *Gpr110*$^{-/-}$ mice (n=10), and control litter mates (n=10). (B) Tumor nodules stripping from nude mice tumor xenograft model, vaccinal tumor tissue masses from wild-type mice. (C) H&E staining of tumor sections from (B) and immunohistochemical staining of AFP in tumor area.

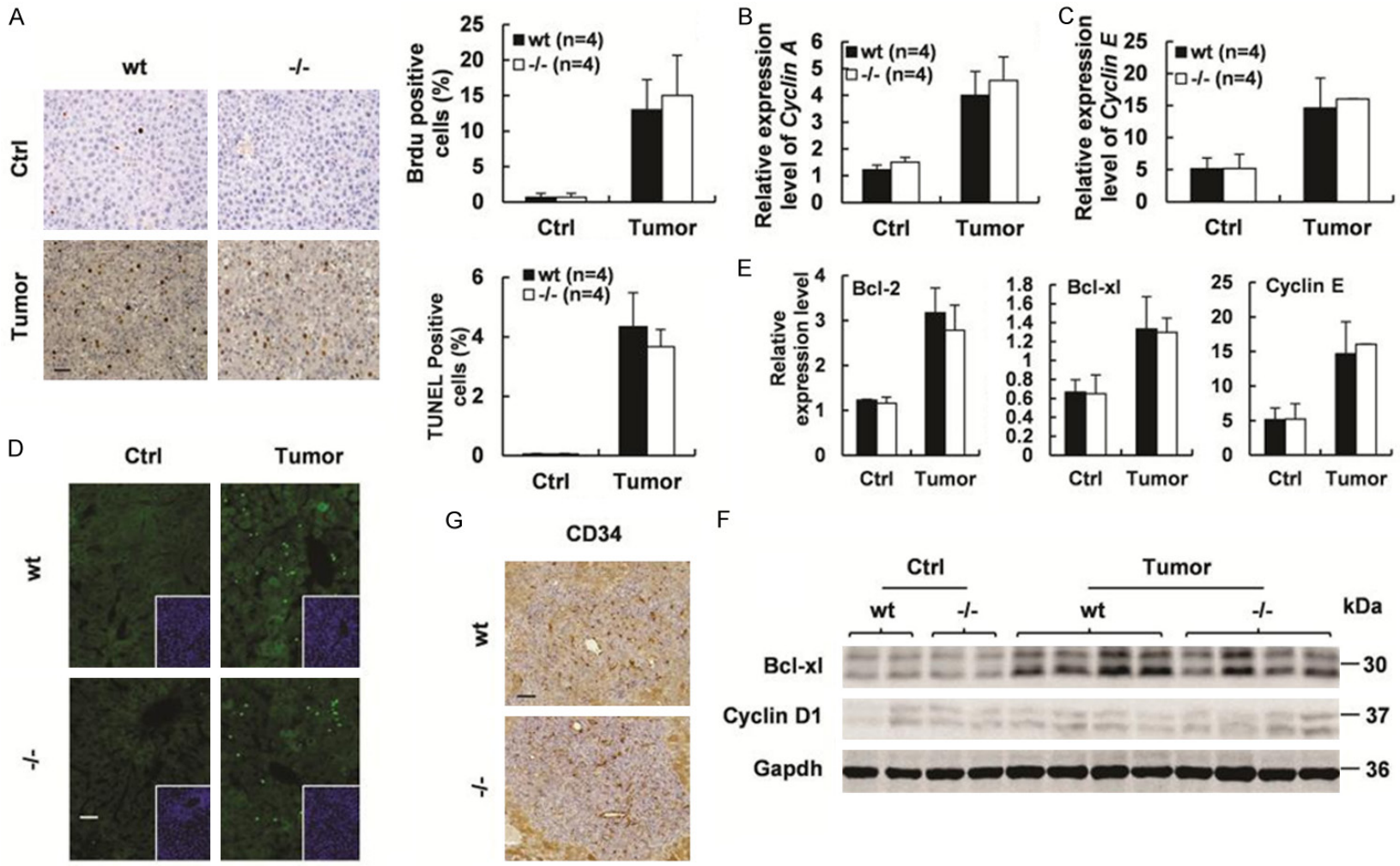

Supplementary Figure 9. Gpr110 did not affect proliferation, apoptosis, or vascularization of tumor in vivo. (A) Immunohistochemical of BrdU in tumor area about liver sections from *Gpr110*$^{-/-}$ mice and wild-type littermates injected with DEN plus CCl_4 after 5 month, quantified by statistical analyzing percentage of positive cells in 20 high-power fields. Scale bar, 50 μm. Values are presented as mean ± SD. **p*<0.05; ***p*<0.01. (B, C) qRT-PCR analyses for *Cyclin A* and *Cyclin E* mRNA expression in liver tumors from (a). Values are presented as mean ± SD from three independent experiments. **p*<0.05; ***p*<0.01. (D) TUNEL staining of liver sections from (A), quantified by statistical analyzing percentage of positive cells in 20 high-power fields. Scale bar, 50 μm. Values are presented as mean ± SD. **p*<0.05; ***p*<0.01. (E) qRT-PCR analyses for *Bcl-2, Bcl-xl,* and *Cyclin E* mRNA expression in liver tumors from (A). Values are presented as mean ± SD from three independent experiments. **p*<0.05; ***p*<0.01. (F) Western blot analysis of Bcl-xl and Cyclin D1 in 5 month CCl_4-treated *Gpr110*$^{-/-}$ mice and wild-type littermate mice liver. (G) Immunostaining of CD34 in the liver sections from (A) (200x). Scale bar, 50 μm.

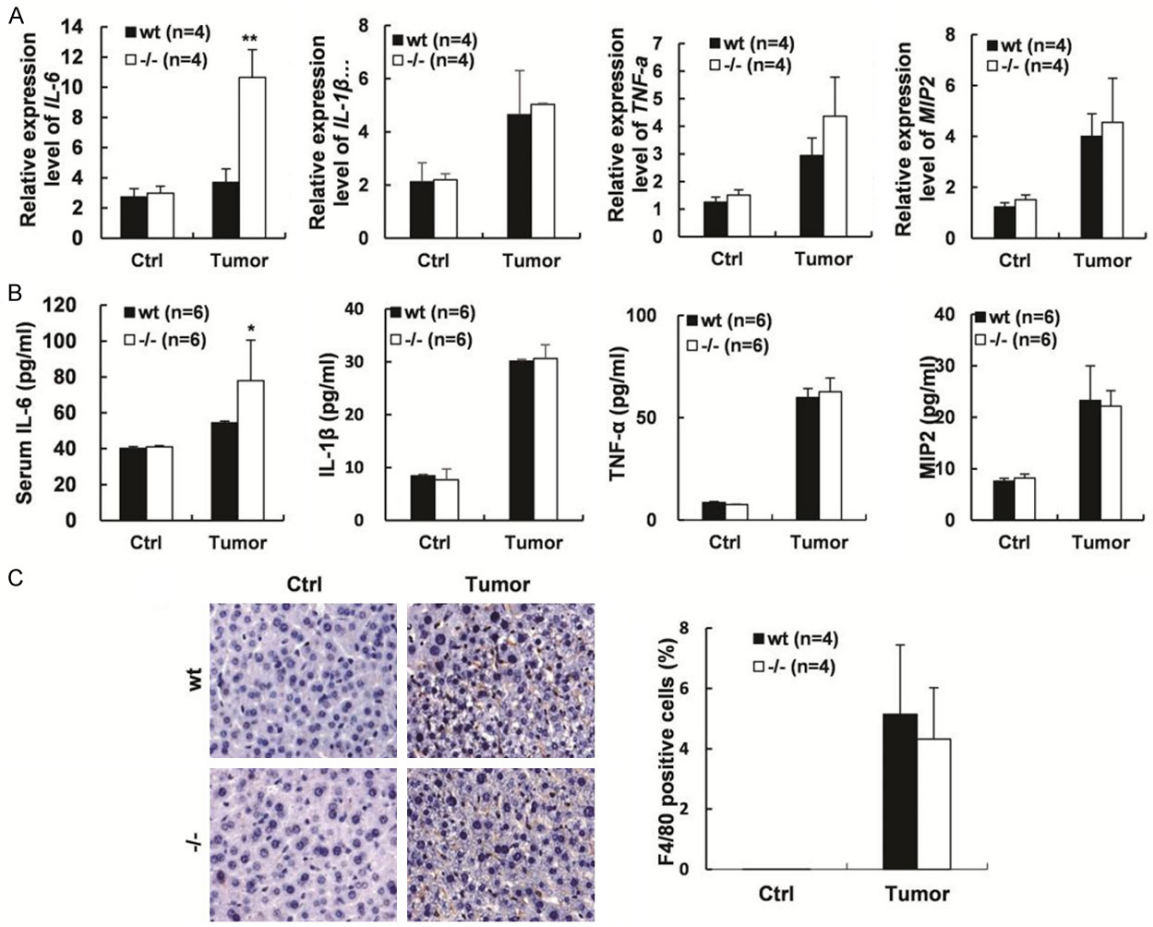

Supplementary Figure 10. Gpr110 did not affect inflammation of tumor induced by CCl_4. A. qRT-PCR analyses for *IL-6*, *IL-1β*, *TNF-α* and *MIP2* mRNA expression in wild-type and *Gpr110*$^{-/-}$ mice liver tumors treated with CCl_4 for 5month (n=4). Values are presented as mean ± SD. **p*<0.05; ***p*<0.01. B. ELISA analysis of serum levels of IL-6, IL-1β, TNF-α and MIP2 in wild-type and *Gpr110*$^{-/-}$ mice liver tumors treated with CCl_4 for 5 month (n=4). Values are presented as mean ± SD. **p*<0.05; ***p*<0.01. C. Immunohistochemical staining of F4/80, sections from *Gpr110*$^{-/-}$ mice and wild-type littermate liver tumors after the CCl_4 injection for 5 month (200×), quantified by statistical analyzing percentage of F4/80 positive cells in 20 high-power fields. Values are presented as mean ± SD. **p*<0.05; ***p*<0.01.

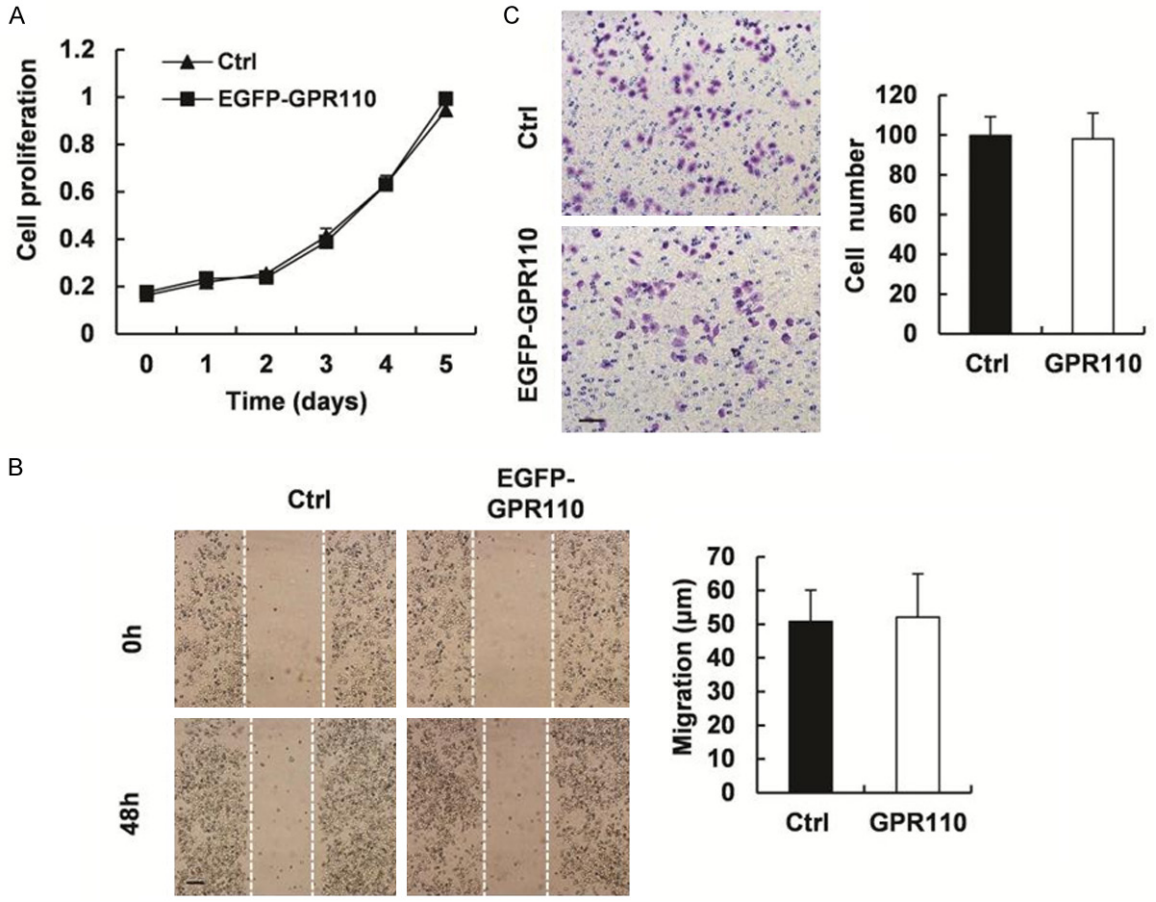

Supplementary Figure 11. Gpr110 had no effect on cell biology function in vitro. A. Cell Counting Kit tested cell proliferation curve in Huh-7 cells after instantaneous overexpression of GPR110. B. Wound-healing assay analysis cell migration ability; migration distance was measured and statistical analyzed. Scale bar, 200 μm. Data shown are means (± SD) from three independent experiments. C. Transwell assay analysis cell migration ability; the cell number was counted and statistical analyzed. Scale bar, 100 μm. Data shown are means (± SD) from three independent experiments.

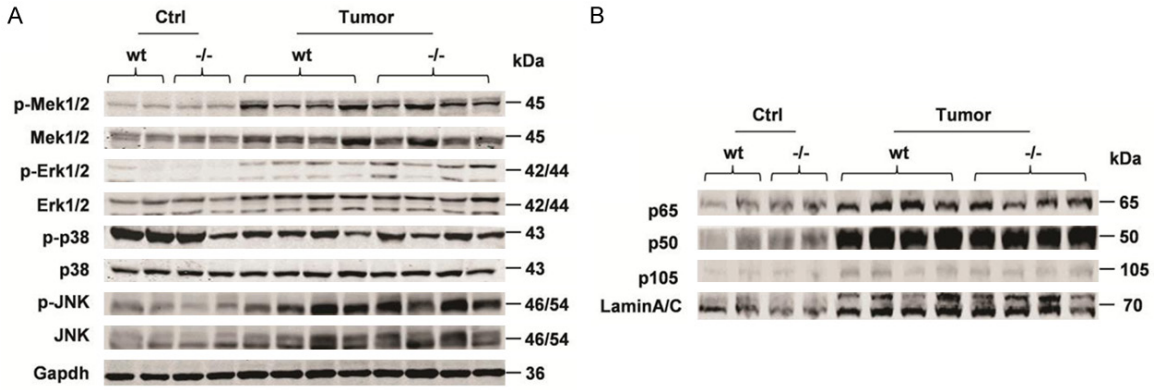

Supplementary Figure 12. Deletion of *Gpr110* did not influence ERK, NF-kB, JNK, or p38/MAPK activation. A. Immunoblot staining analysis of p-Mek1/2, Mek1/2, p-Erk1/2, Erk1/2, p-p38, p38, p-JNK, JNK, in olive oil and DEN plus CCl_4-treated 5 month *Gpr110*$^{-/-}$ mice and wild-type littermate mice liver (n=6). B. Immunoblot staining analysis of nuclear levels of p65, p50, and p105 in olive oil and DEN plus CCl_4-treated 5 month *Gpr110*$^{-/-}$ mice and wild-type littermate mice liver (n=6).